NACA RM E52H26

NACA

RESEARCH MEMORANDUM

EFFECT OF GEOMETRY ON SECONDARY FLOWS IN BLADE ROWS

By A. G. Hansen, G. R. Costello, and H. Z. Herzig

Lewis Flight Propulsion Laboratory
Cleveland, Ohio

NATIONAL ADVISORY COMMITTEE
FOR AERONAUTICS
WASHINGTON
October 16, 1952

1L

2696

NATIONAL ADVISORY COMMITTEE FOR AERONAUTICS

RESEARCH MEMORANDUM

EFFECT OF GEOMETRY ON SECONDARY FLOWS IN BLADE ROWS

By A. G. Hansen, G. R. Costello, and H. Z. Herzig

SUMMARY

The influence of blade-row geometry on secondary flows in a two-dimensional cascade was investigated qualitatively by varying independently stagger angle, aspect ratio, solidity, and angle of attack and by providing blade fillets. The influence of tip clearance and relative motion between blades and wall was also studied.

Stagger angle and aspect ratio had no appreciable effect on this secondary flow, whereas solidity and angle of attack did affect the flow patterns indicating the turning as a major parameter.

Blade-tip clearance induced a vortex, produced by flow under the blade end, which rotated opposite to the original secondary flow passage vortex. The clearance vortex displaced but did not reduce the secondary flow vortex.

When the wall was moved relative to the blades, the blade leading surfaces "scraped" up entrained fluid near the wall and imparted a roll-up motion to the air in this region. On the trailing surface the fluid was pulled off the blade onto the wall. The magnitude of the scraping effect was so large that it completely masked the secondary flow and tip clearance phenomena.

INTRODUCTION

An important problem arising in the design of turbomachines and in the analysis of their performance is an understanding of the nature and influence of so-called secondary flows. Unfortunately, because of complicated three-dimensional flow patterns, it is difficult to arrive at an understanding of the secondary flows in a turbomachine by instituting the study of such flows directly in the machine. Accordingly, as a first step in attempting to analyze secondary flows, visualization techniques were used to obtain the streamline patterns in a stationary two-dimensional cascade (reference 1).

The streamlines of the wall boundary layer at the inlet were observed (reference 1) to deflect across the passage to the blade suction

surface and to form a vortex well upstream of the blade trailing edge.
In addition to crossing the passage, some of these streamlines deflected
away from the wall as well, and all the streamlines flowed together in
a small region at approximately the same axial location to form the vor-
tex. It was further shown that over a wide range the free-stream veloc-
ity had little or no effect on this pattern of boundary-layer deflec-
tions.

Because this combination of cross-channel and away-from-the-wall
deflection of the boundary layer is a three-dimensional phenomenon
resulting in the formation of the passage vortex, the concepts of two-
dimensional analysis cannot be applied in order to predict the behavior
of these secondary flow patterns. For this reason it was impossible to
extend the foregoing study to more general configurations by two-
dimensional analysis and therefore the influence of blade geometry on
secondary flows was investigated qualitatively at the NACA Lewis labor-
atory by independently varying stagger angle, aspect ratio, solidity,
and angle of attack and by use of blade fillets in the cascade of refer-
ence 1. Furthermore, in order to simulate more closely the conditions
in a turbomachine, the cascade was modified to enable the study of the
influence of tip clearance and relative motion between wall and blades.
Flow visualization by smoke traces was used to determine the streamline
patterns for the various configurations and the results are presented
herein.

                              PROCEDURES

In order to study the influence of blade geometry on secondary
flows in two-dimensional cascades, the cascade of reference 1 was modi-
fied for the investigation of the following numerical values of param-
eters in addition to those already reported in reference 1 (the paren-
thetical values were presented in reference 1): stagger angle, 0°
(45°); aspect ratio, 1.67 (2.34); solidities, 2.0 (1.5), and 0.75;
angles of attack, 4°, 7° (11°), 15°, and 20°. Also, blade fillets
were added on the suction surface, on the pressure surface, and on both
blade surfaces, respectively, to evaluate their effects on the secondary
flows.

In order to simulate more closely the conditions in a turbomachine,
tip clearances of 0.060 and 0.014 inches were provided. One of the
end walls of the cascade was then replaced by an endless moving belt
whose direction and speed could be varied in order to study the influ-
ence of relative motion between blades and wall.

The tests were conducted with three belt speeds; slow speed (belt
speed approximately one-half air speed), medium speed (belt speed

approximately equal to air speed), and high speed (belt speed well above air speed).

The case where the direction of motion of the wall is such that the pressure surface is the leading surface resembles the relative motion between blades and wall in an axial-flow compressor. When the belt direction is reversed, the relative motion between blades and wall resembles that in the turbine rotor.

For convenience, in the course of making the modifications to the cascade as required for the geometric configurations under study, various lengths of inlet section, constructed of different materials, were used because preliminary checks showed (within wide limits) that the thickness of the inlet boundary layer did not affect the type of results obtained. In each case with the main stream velocity about 30 feet per second, the secondary-flow patterns were observed by the flow-visualization techniques using smoke, as described in reference 1.

RESULTS AND DISCUSSION

The details of the formation of a passage vortex as a result of the deflection of the inlet boundary layer across the passage to the blade suction surface, together with deflections away from the wall of portions of this inlet boundary layer, are described in reference 1. This phenomenon is shown in figure 1.

Following are results showing how variations in cascade geometry affect this secondary-flow picture.

Stagger angle. - The deflections of the streamlines in the inlet boundary layer which join in a region near the suction surface is demonstrated in figures 2(a) to 2(c), for a cascade with a stagger angle of 0° (where stagger angle is the angle between cascade axis and incoming air). In each case, the values of the parameters are given in the legend. This streamline pattern can be seen, by comparison, to be essentially identical with the pattern in figure 1, where the stagger angle is 45°.

The path of a streamline in the main flow through the cascade with a stagger angle of 0° is shown in figure 2(d). The turning of the flow is essentially unchanged from that of the cascade with a stagger angle of 45° of reference 1.

Aspect ratio. - The aspect ratio for the two-dimensional cascade was reduced from 2.34 to 1.67 by means of specially devised inserts along the end walls. The boundary-layer streamlines (fig. 3) remain

unaffected. It was observed that the spanwise deflection of corresponding streamlines in the boundary layer was also unaffected by the change in aspect ratio.

Solidity. - With the solidity reduced from 1.5 to 0.75, the main portion of the inlet boundary-layer streamline at a blade nose was not deflected completely across the channel (fig. 4(a)). Most of the smoke was deflected part way across and then proceeded downstream. The wisp of smoke seen at the trailing edge reached there by flowing upstream in the separated region behind the suction surface of the blade. In the case with the solidity reduced to 0.75, it was observed that the three-dimensional aspects of the boundary-layer flow, namely the deflection of streamlines near the suction surface in a direction away from the wall, had decreased considerably and the passage vortex was smaller. Because the camera shows only projections, the deflections away from the wall could not be photographed here. Consequently, the photographs show only cross-channel deflection but the three-dimensional aspects of the flow cannot be ignored for proper interpretation of the phenomena reported.

The streamline at the first probe location at which the suction surface was reached by cross-channel flow is shown in figure 4(b). The turning of the mean stream (fig. 4(c)) is less at the low solidity of 0.75 than at the design solidity of 1.5 (fig. 2(d)).

The results of tests at solidity of 2.0 are shown in figure 5. Figure 5(a) shows, as might be expected, that the boundary-layer streamline at the nose of one blade is deflected all the way across the channel. The main stream flow (fig. 5(b)) is turned somewhat more than in the design case (solidity 1.5).

Angle of attack. - The streamline patterns for the cascade at design solidity of 1.5 and at angles of attack of 4°, 7°, 15°, and 20° (design angle of attack is presented in reference 1) are shown in figures 6 to 9, respectively. As the angle of attack increased, the cross-channel and away-from-the-wall deflection increased, and the passage vortex became larger.

Combined solidity and angle of attack. - The streamline paths for the cascade with solidity of 0.75 and angle of attack of 4° are shown in figure 10. It is necessary to come almost half-way across the channel at the inlet in order to find a streamline which is deflected to the suction surface. It was observed that in this case the deflections away from the wall were smaller than for the design configuration. At a solidity of 2.0 and an angle of attack of 20° (fig. 11), with the probe away from the wall, some streamlines in the blade boundary layer up on the pressure surface of the blade deflect to the wall and there cross

2696

the channel to the suction surface to comprise part of the passage vortex. A comparison of the amount of turning of the main streams for the two configurations, which represent the extremes of the ranges investigated, is possible with the use of figures 10(c) and 11(b).

This study of solidities and angles of attack indicates that the over-all turning as well as the local turning of the main streams of the blade rows are major factors in the cross-channel and spanwise deflection of the inlet wall boundary layer. Furthermore, it was observed during these tests that for the configurations which involved greater turning, the spanwise deflection of the corresponding streamlines in the boundary layers increased, the roll up into the passage vortex was "tighter", and the vortex was larger.

Blade fillets. - Fillets of approximately 3/16-inch radius of curvature on the blade pressure surface, blade suction surface, and on both blade surfaces are shown in figures 12(a), 12(b), and 12(c), respectively. As can be seen from the figures, none of these fillets prevented the typical secondary-flow vortex from forming in the passage. Similar results were obtained with larger fillets, as well.

Tip clearance. - The possibility that blade tip clearance in turbomachines alleviates secondary-flow losses has been suggested. This was not confirmed from flow patterns obtained in cascades having blade tip clearances of 0.060 and 0.014 inch (1.7 percent and 0.4 percent span, respectively). The patterns for these clearances are shown in figures 13 and 14. The point of principal interest arising from this study was the fact that with tip clearance the passage vortex heretofore observed was displaced, but was neither eliminated nor apparently reduced in magnitude.

The deflection of the flow along the pressure surface is greater than for blades without tip clearance because a large part of the flow under the blade tip comes from flow off the blade pressure surface as shown in figure 13(a). For this particular probe location, the flow was observed to cross under the blade tip at the midchord position. This blade boundary-layer flow, which crosses under the blade, forms a vortex lying against the suction surface. This tip-clearance vortex rotates in a direction opposite to that of the secondary-flow vortex and preempts the region where the secondary-flow vortex would form if no tip clearance were present. Nevertheless, figure 13(b) shows that the usual passage vortex still exists and is merely displaced by the tip-clearance vortex.

Essentially the same phenomenon for 0.060-inch blade-tip clearance and for a cascade stagger angle of 45° is illustrated in figures 14(a) to 14(c). The tip-clearance vortex in figure 14(a) was traced out by

smoke admitted through a probe. Figure 14(b) is a side view of the displaced passage vortex and was obtained when the smoke was admitted through wall static taps upstream of the blades. Figure 14(c) depicts the pattern obtained from smoke admitted through the probe to give the tip-clearance vortex, while smoke is admitted simultaneously through a wall static tap to give the usual secondary-flow vortex. The manner in which the tip-clearance vortex flows concomitantly with and contiguous to the secondary-flow vortex can be clearly seen.

A particularly striking picture of the tip-clearance vortex formed in a cascade with a stagger angle of 0° and a 0.060-inch blade clearance is shown in figure 14(d).

Relative motion between blades and wall. - The investigation of the flow behavior when relative motion existed between the cascade blades and the cascade end wall disclosed some unexpected results. In particular, it had been assumed apriori that the moving wall would tend to increase the flow of the wall boundary layer as well as of the blade boundary layer off the leading surface and to pull them under the blade tips in the direction of the wall motion, however, figure 15 indicates that this assumption is invalid. Comparison of smoke deflection in figure 15(a), where the wall is stationary, with figures 15(b) and 15(c), where the motion of the wall is such to make the pressure surface the "leading" surface, shows that flow on the blade is actually deflected away from the wall. Similarly, figure 16 where the suction surface is leading shows increased deflection of the flow away from the wall with increasing wall speed; figures 16(a), (b), and (c), illustrate the patterns for the wall stationary, the wall moving at moderate speed, and the wall moving at high speed, respectively.

The explanation of the observed phenomenon is that the blades have a scraping action on the flow near the moving wall. The blade leading surface scrapes up fluid entrained on the moving wall thus imparting a rolling motion to the air in the vicinity of the leading surface. Figure 17 shows this roll up when the pressure surface is leading. Figure 18 portrays the same type of roll up when the suction surface is leading. One consequence of this scraping effect is that the tip-clearance vortex associated with a stationary wall (figs. 13 and 14) is now virtually eliminated.

The patterns on the pressure surface of a blade when the suction surface is leading are shown in figure 19. In a comparison of the flow deflection in figure 19(a), wall stationary, with figures 19(b) and 19(c), wall moving, the wall motion increases the flow deflection toward the wall. Smoke injected near the moving wall actually flowed down the blade and onto the wall and was carried across to the adjacent blade suction surface.

Similarly, figure 20 shows that the moving wall, with the pressure surface leading, deflects the flow on the suction surface toward the wall. In this case, it was also observed that smoke flowed down the blade, onto the wall, and was carried over to the pressure surface of the adjacent blade. A photograph of this effect was unobtainable because of the severe diffusion that existed when smoke was so introduced. Furthermore, this action of the moving wall with the pressure surface leading removed the stagnant air region previously existing on the blade suction surface near the trailing edge so that the flow remained attached to the entire blade suction surface.

CONCLUDING REMARKS

Throughout the investigation of various geometric configurations of the two-dimensional cascade, the basic mechanism of the formation of a secondary-flow passage vortex was unchanged; however, the degree to which the wall boundary layer deflected away from the wall and across the channel and the size and "tightness" of the passage vortex were influenced by those parameters which involved the turning of the main flow, and the local pressure gradients in the wall boundary layer. These parameters, as illustrated by the figures, were solidity and angle of attack. Parameters, such as aspect ratio and stagger angle, that did not alter the turning had no apparent influence on this secondary flow. Furthermore, the presence of fillets on the blades did not prevent the passage vortex roll up.

Instead of reducing secondary-flow effects, tip clearance resulted in merely displacing the secondary-flow vortex and provided another vortex rotating in the opposite direction. The two vortices rotated side by side without much mixing, and thus constituted a considerably larger flow disturbance than did the secondary flows alone.

With the wall moving past the blade ends, the net effect was that flow near the wall was scraped off and was rolled up by the blade leading surfaces, while the low-momentum fluid on the blade trailing surfaces was pulled off the blades.

In the case where the pressure surface was leading, as for example in a compressor, this behavior acted: (a) to improve generally the tip flow on the pressure surface in the sense that it prevented the tip flow from deflecting under the blade and forming a vortex and thus improved the blade loading characteristics near the tip; (b) to improve flow characteristics on the blade suction surface even at some spanwise distance from the tip by reducing or eliminating the "dead" region which exists when the wall is stationary; and (c) to replace the secondary-flow vortex and tip-clearance vortex by a different roll up near the blade leading surface. The patterns of the flow obtained with the

pressure surface leading simulate, to a degree, the absolute fluid motion in an axial-flow-compressor stator, or the relative motion in the compressor rotor.

When the suction surface was leading, this behavior acted: (a) to aggravate the tip effects at the pressure surface by increasing the deflection of the flow and thereby impairing the blade loading characteristics at the tip; and (b) to aggravate the effects at the suction surface by piling up fluid there to increase the secondary-flow effects while adding a new roll up near the leading surface. In this case with the suction surface leading, the flow patterns simulate, to a degree, the relative motion of the fluid at the blade tips of a turbine rotor.

The foregoing observations offer possible explanation for the larger tip losses encountered in turbines as compared with compressors.

Lewis Flight Propulsion Laboratory
        National Advisory Committee for Aeronautics
                Cleveland, Ohio

<div align="center">REFERENCE</div>

1. Herzig, H. Z., Hansen, A. G., and Costello, G. R.: Visualization of Secondary-Flow Phenomena in Blade Row. NACA RM E52F19, 1952.

Figure 1. - Deflection of streamlines in wall boundary layer at inlet showing passage
  vortex formation. Solidity, 1.5; angle of attack 11°; stagger angle, 45°; aspect
  ratio, 2.34.

(a) Probe on wall near pressure surface.
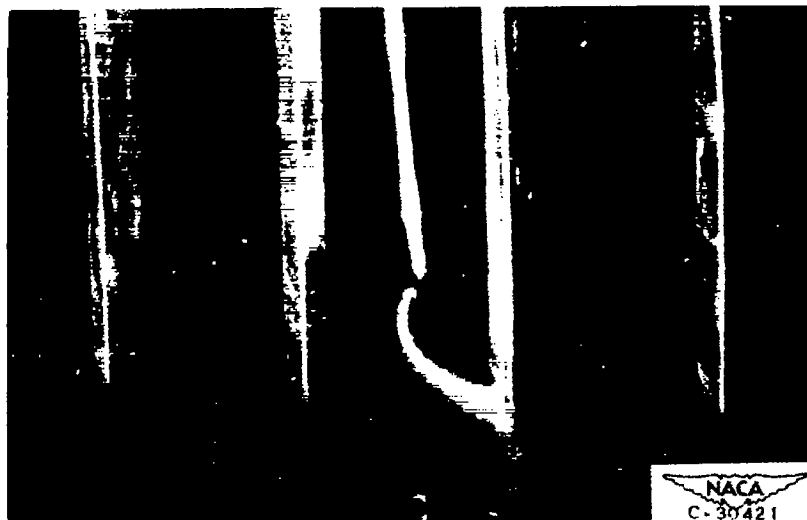
(b) Probe on wall in midchannel.

Figure 2. - Streamline pattern in cascade with stagger angle of 0°. Solidity, 1.5; angle of attack, 11°; aspect ratio, 2.34.

2696

(c) Probe on wall near suction surface.

(d) Probe away from wall in main stream.

Figure 2. - Concluded.　Streamline pattern in cascade with stagger angle of 0°.　Solidity, 1.5; angle of attack, 11°; aspect ratio, 2.34.

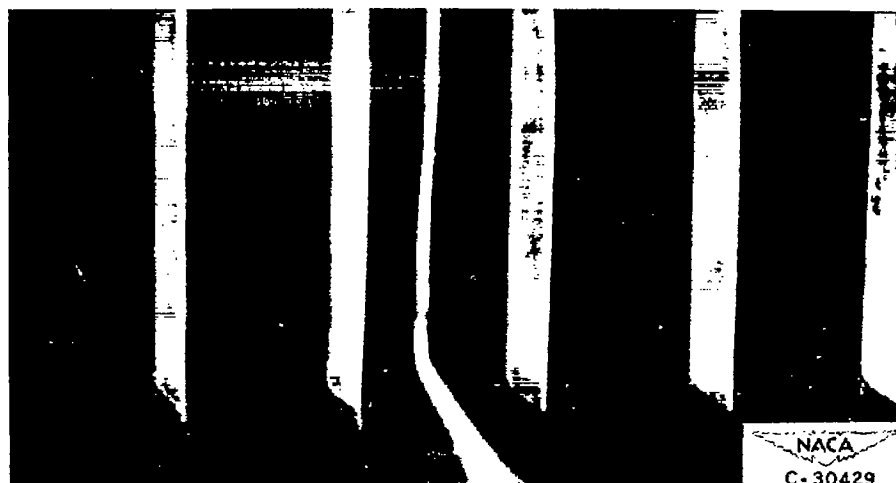(a) Probe on wall at nose of blade.
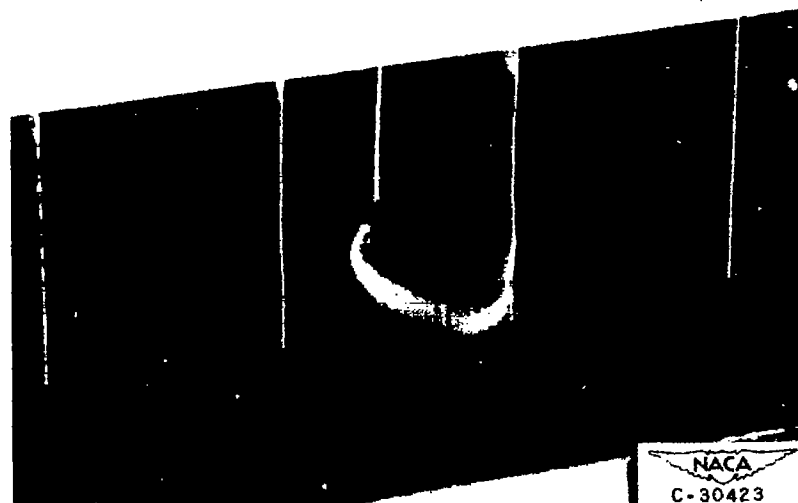
(b) Probe on wall near pressure surface.

Figure 3. - Streamline pattern in cascade with aspect ratio of 1.67. Stagger angle, 45°; solidity, 1.5; angle of attack, 11°.

2696

(c) Probe on wall near suction surface.

Figure 3. - Concluded. Streamline pattern in cascade with aspect ratio of 1.67. Stagger angle, 45°; solidity, 1.5; angle of attack, 11°.
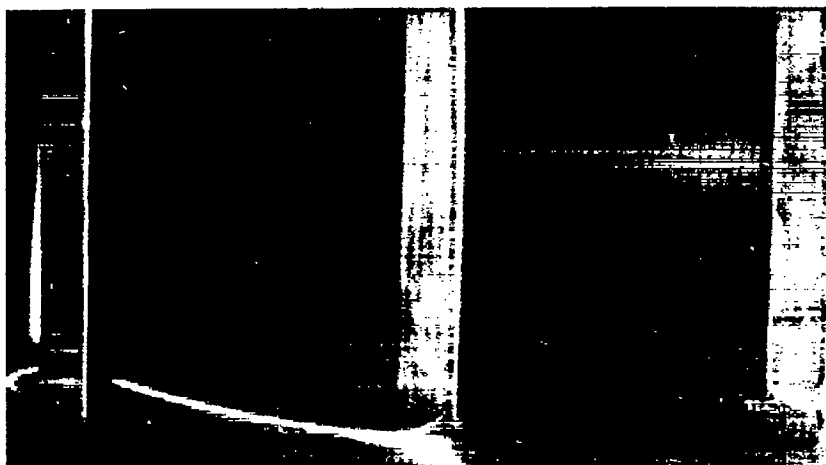
(a) Probe on wall at nose of blade.

(b) Probe on wall at point where smoke first reached suction
surface.

Figure 4. - Streamline pattern in cascade with solidity of 0.75. Stagger angle, 0°;
angle of attack, 11°; aspect ratio, 2.34.

(c) Probe away from wall in main stream.

Figure 4. - Concluded. Streamline pattern in cascade with solidity of 0.75. Stagger
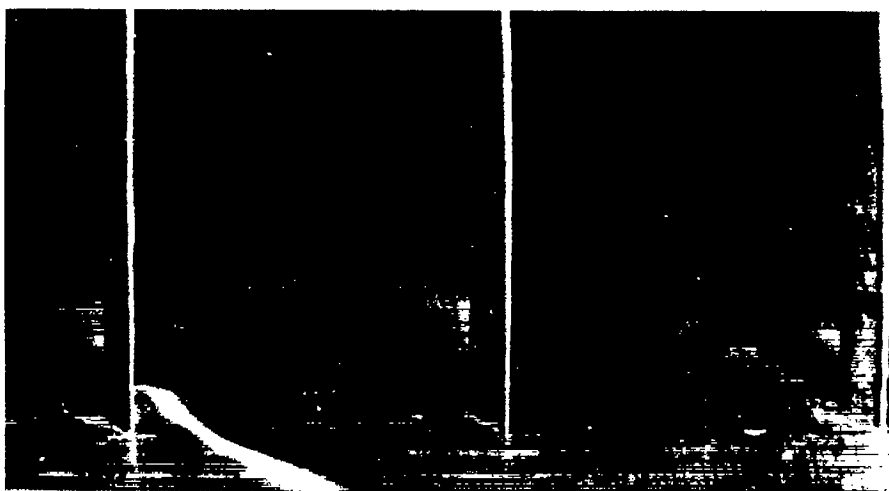angle, 0°; angle of attack, 11°; aspect ratio, 2.34.
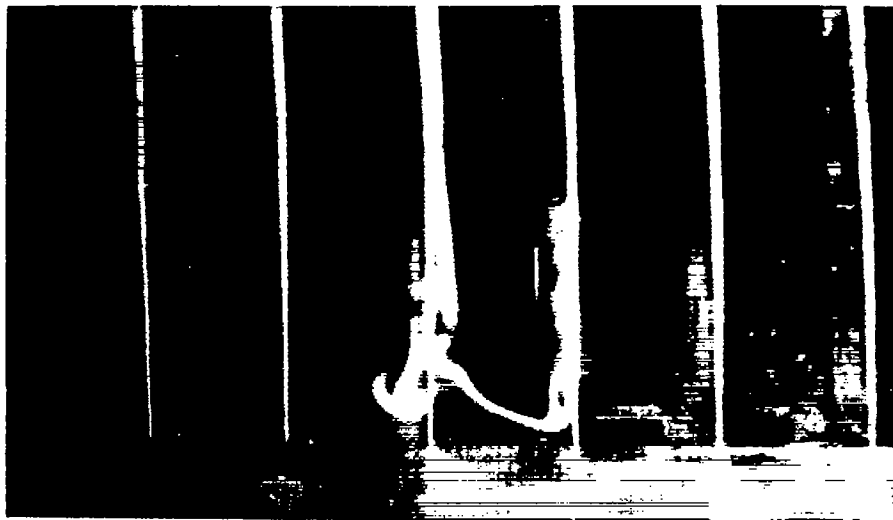
(a) Probe on wall at nose of blade.

(b) Probe away from wall in main stream.

Figure 5. - Streamline pattern in cascade with solidity of 2.0. Stagger angle, 0°;
angle of attack, 11°; aspect ratio, 2.34.

(a) Probe on wall at nose of blade.

(b) Probe on wall at point where smoke first reached suction
surface.

Figure 6. - Streamline pattern in cascade with angle of attack of 4°. Stagger angle, 0°;
solidity, 1.5; aspect ratio, 2.34.

(c) Probe away from wall in main stream.

Figure 6. - Concluded.   Streamline pattern in cascade with angle of attack of 4°.   Stagger
angle, 0°; solidity, 1.5; aspect ratio, 2.34.
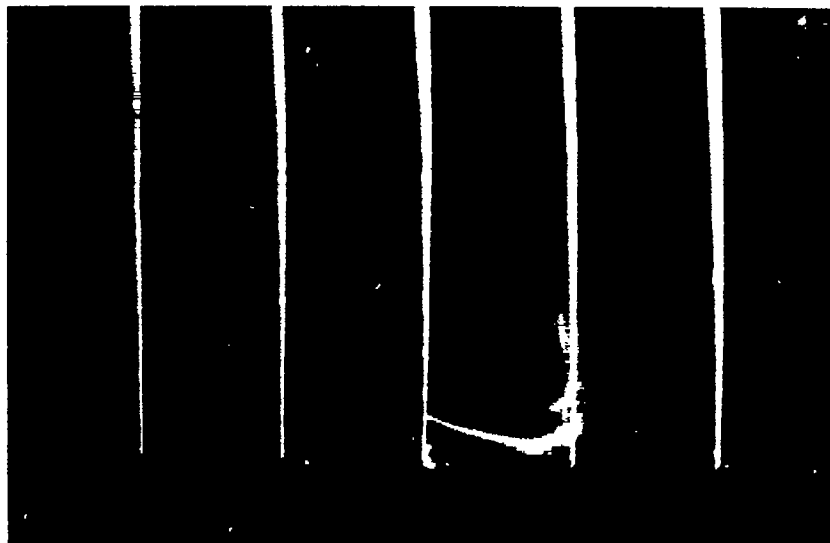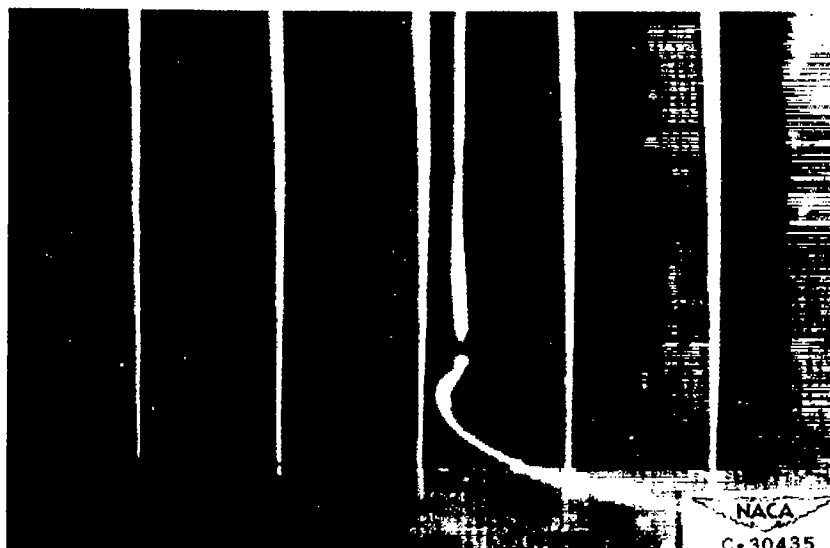
2696

(a) Probe on wall at nose of blade.

(b) Probe away from wall in main stream.

Figure 7. - Streamline pattern in cascade with angle of attack of 7°. Stagger angle, 0°; solidity, 1.5; aspect ratio, 2.34.
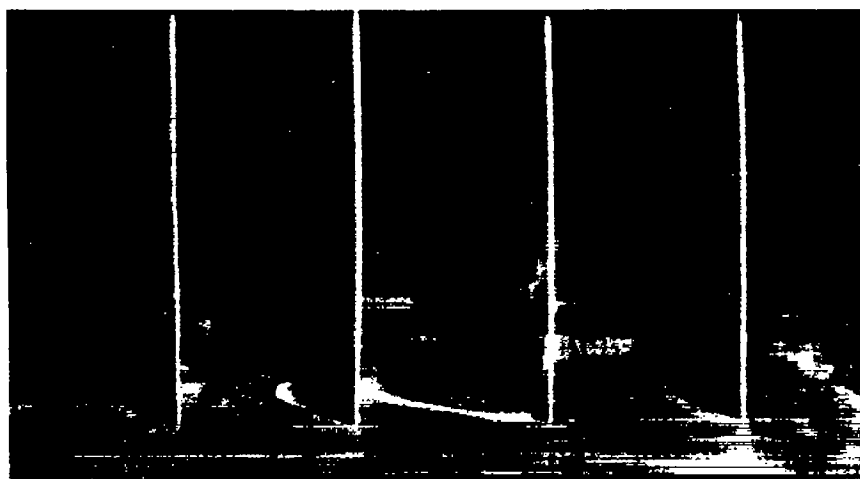
(a) Probe on wall at nose of blade.

(b) Probe away from wall in main stream.

Figure 8. - Streamline pattern in cascade with angle of attack of 15°. Stagger angle, 0°; solidity, 1.5; aspect ratio, 2.34.

2696

(a) Probe on wall at nose of blade.

(b) Probe away from wall in main stream.

Figure 9. - Streamline pattern in cascade with angle of attack of 20°. Stagger angle, 0°; solidity, 1.5; aspect ratio, 2.34.

(a) Probe on wall at nose of blade.

(b) Probe on wall at point where smoke first reached suction
surface.

Figure 10. - Streamline pattern in cascade with solidity of 0.75 and angle of attack
of 4°. Stagger angle, 0°; aspect ratio, 2.34.

2696

(c) Probe away from wall in main stream.

Figure 10. - Concluded. Streamline pattern in cascade with solidity of 0.75 and angle of attack of 4°. Stagger angle, 0°; aspect ratio, 2.34.

2696

(a) Probe away from wall at nose of blade.

(b) Probe away from wall in main stream.

Figure 11. - Streamline pattern in cascade with solidity of 2.0 and angle of attack of 20°. Stagger angle, 0°; aspect ratio, 2.34.

4L

2696

(a) Fillet on blade pressure surface.

(b) Fillet on blade suction surface.

Figure 12. - Streamline pattern in cascade with blade fillets. Stagger angle, 0°; angle of attack, 11°; solidity, 1.5; aspect ratio, 2.34.
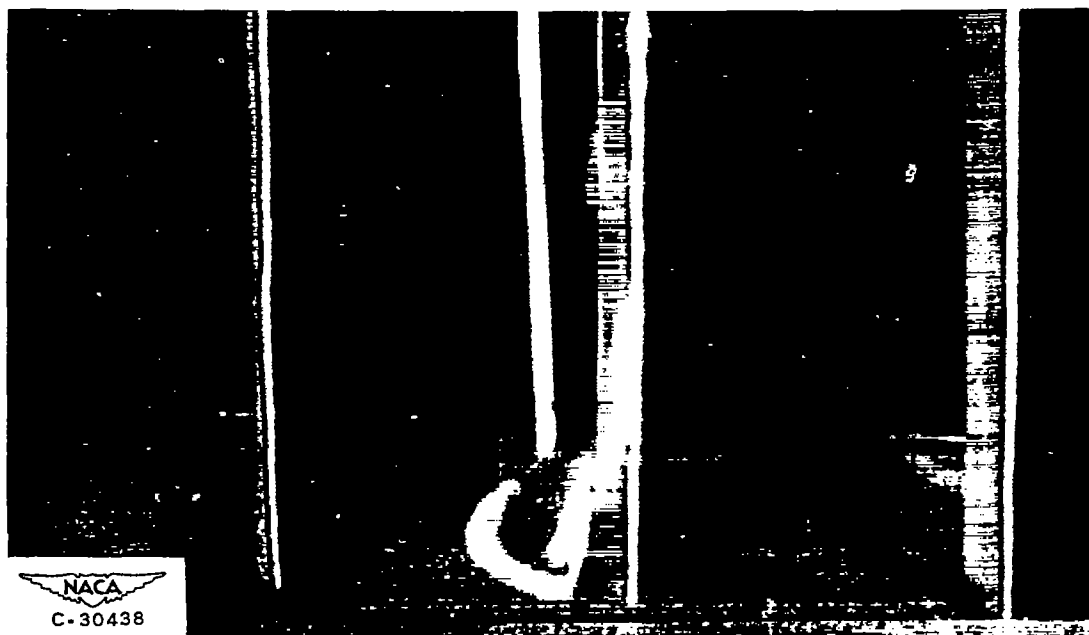
(c) Fillets on both blade surfaces.

Figure 12. - Concluded. Streamline pattern in cascade with blade fillets. Stagger angle, 0°; angle of attack, 11°; solidity, 1.5; aspect ratio, 2.34.

2696
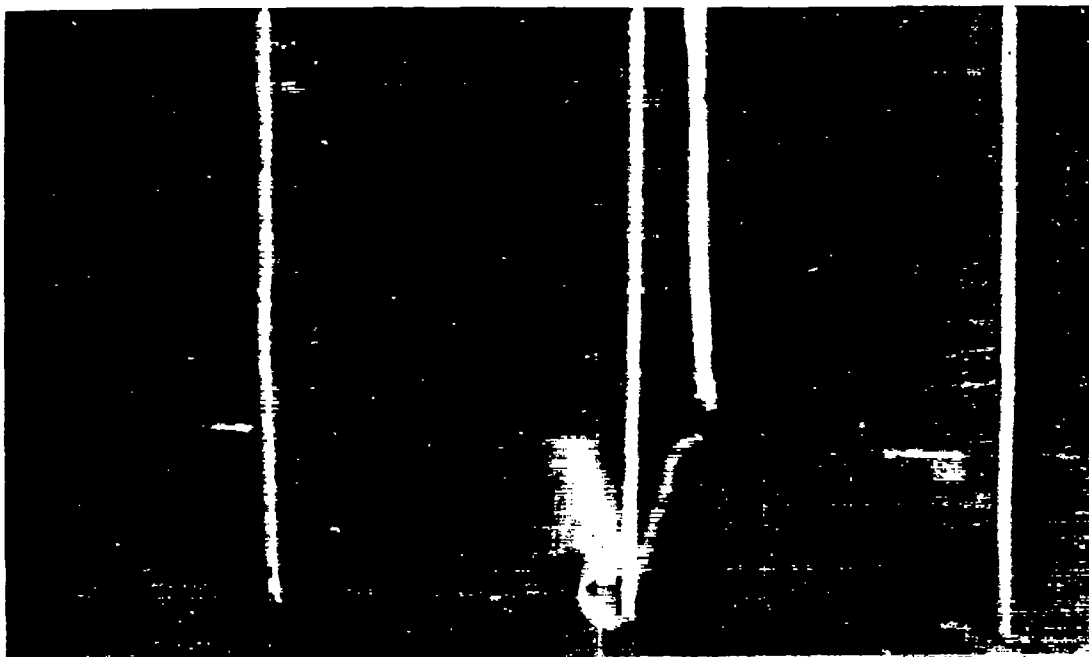
(a) Probe away from wall on nose of blade.

(b) Probe on wall in midchannel.

Figure 13. - Streamline pattern in cascade with 0.014 blade tip clearance. Stagger angle,
0°; angle of attack, 11°; solidity, 1.5; aspect ratio, 2.34.

(a) Probe on wall near nose of blade. Stagger angle, 45°.

(b) Static taps near nose of blade and in midchannel.
Stagger angle, 45°.

Figure 14. - Streamline patterns for cascade with 0.060-inch blade tip clearance.
Solidity, 1.5; angle of attack, 11°; aspect ratio, 2.34.

(c) Static tap near nose of blade and probe or wall near nose of blade.
Stagger angle, 45°.

(d) Probe away from wall on nose of blade.
Stagger angle, 0°.

Figure 14. - Concluded. Streamline patterns for cascade with 0.060-inch blade end
clearance. Solidity, 1.5; angle of attack, 11°; aspect ratio, 2.34.

2696

(a) Probe on nose of blade; stationary wall.

(b) Probe on nose of blade; moderate speed wall.

Figure 15. - Streamline deflections on pressure surface of blade. Pressure surface
leading; 0.014-inch blade end clearance; stagger angle, 0°; solidity, 1.5; angle of
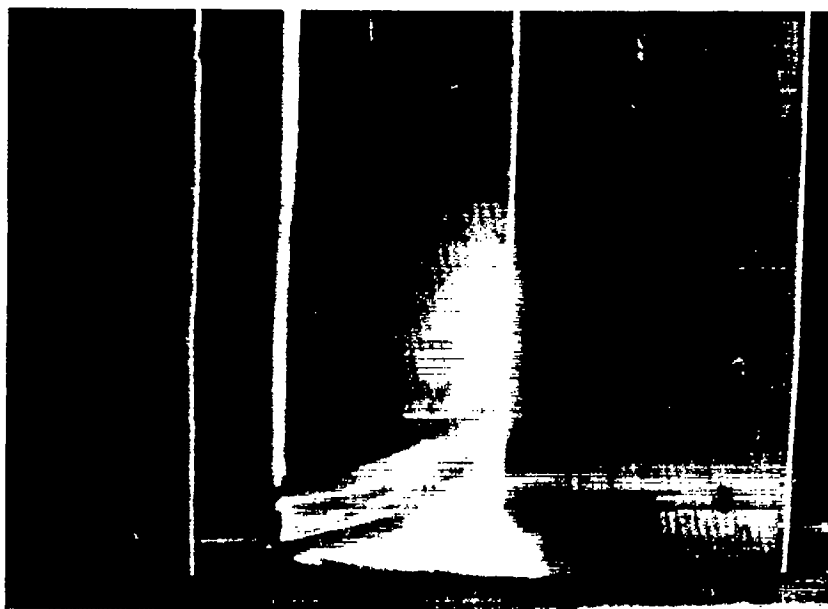attack, 11°; aspect ratio, 2.34.

(c) Probe on nose of blade, high-speed wall.

Figure 15. - Concluded. Streamline deflections on pressure surface of blade. Pressure
   surface leading; 0.014-inch blade end clearance; stagger angle, 0°; solidity, 1.5;
   angle of attack, 11°; aspect ratio, 2.34.
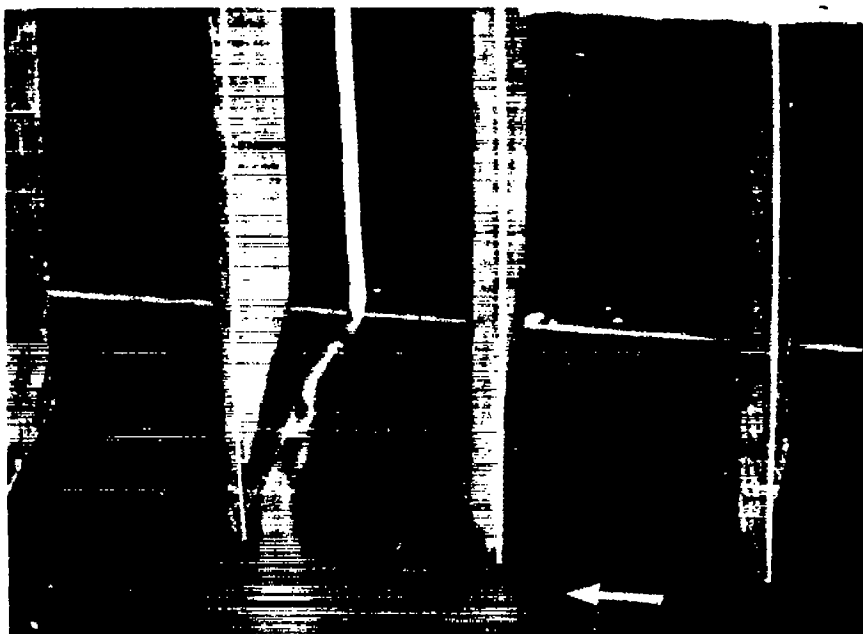
(a) Probe on nose of blade; stationary wall.

(b) Probe on nose of blade; moderate speed wall.

Figure 16. - Streamline deflections on suction surface of blade. Suction surface lead-
ing; 0.014-inch blade end clearance; stagger angle, 0°; solidity, 1.5; angle of attack,
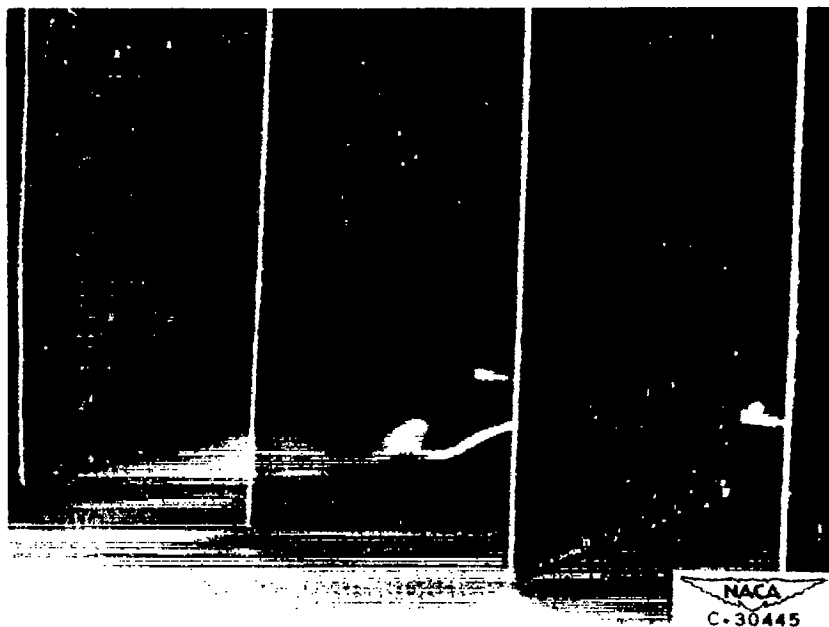11°; aspect ratio, 2.34.

(c) Probe on nose of blade; high-speed wall.

Figure 16. - Concluded. Streamline deflections on suction surface of blade. Suction
  surface leading; 0.014-inch blade end clearance; stagger angle, 0°; solidity, 1.5;
  angle of attack, 11°; aspect ratio, 2.34.

(a) Probe near pressure surface of blade; moderate speed wall.

(b) Probe near pressure surface of blade; moderate speed wall.

Figure 17. - Streamline patterns showing scraping effect of blade. Pressure surface
leading; 0.014-inch blade end clearance; stagger angle, 0°; solidity, 1.5; angle of
attack, 11°; aspect ratio, 2.34.

Figure 18. - Streamline patterns showing scraping effect of blade; suction surface
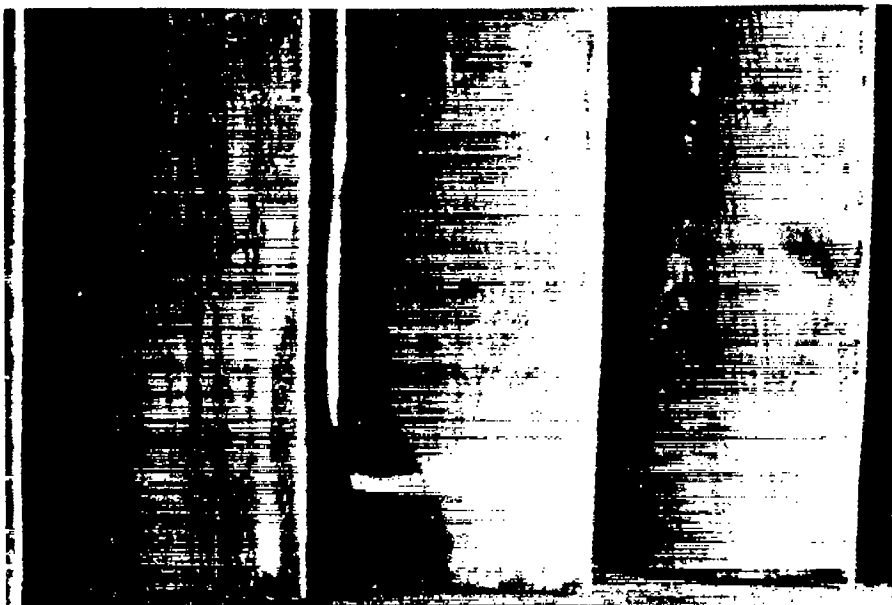leading.

(a) Probe on nose; stationary wall.

(b) Probe on nose; slow-speed wall.

Figure 19. - Streamline deflections on pressure surface of blade. Suction surface
leading; 0.014-inch blade end clearance; stagger angle, 0°; solidity, 1.5; angle
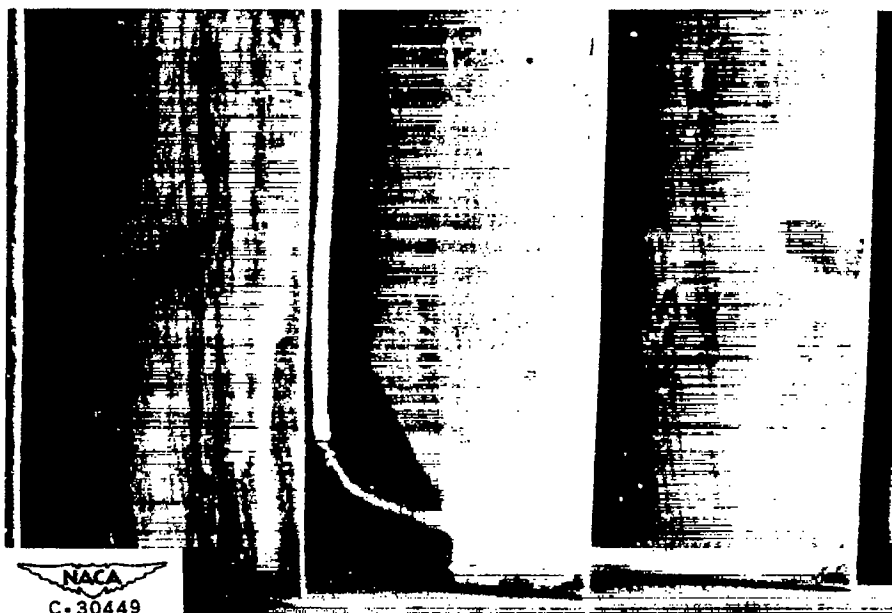of attack, 11°; aspect ratio, 2.34.

(c) Probe on nose; high-speed wall.

Figure 19. - Concluded. Streamline deflections on pressure surface of blade. Suction
surface leading; 0.014-inch blade end clearance; stagger angle, 0°; solidity, 1.5;
angle of attack, 11°; aspect ratio, 2.34.

(a) Probe on nose; stationary wall.

(b) Probe on nose; moderate speed wall.

Figure 20. - Streamline deflection on suction surface of blade. Pressure surface
leading; 0.014-inch blade-end clearance; stagger angle, 0°; solidity, 1.5; angle
of attack, 11°; aspect ratio, 2.34.